Earthquakes and Structures, *Vol. 12, No. 1 (2017) 177-189*
DOI: https://doi.org/10.12989/eas.2017.12.1.177

A simplified normalized cumulative hysteretic energy spectrum

Guohua Sun*, Qiang Gu and Youzhen Fang

School of Civil Engineering, Suzhou University of Science and Technology, Suzhou, Jiangsu, 215011, China

(Received June 17, 2016, Revised November 7, 2016, Accepted December 25, 2016)

Abstract. For energy-based seismic design, a simplified normalized cumulative hysteretic energy spectrum proposed for obtaining hysteretic energy as energy demand is the main objective in this paper. The dimensionless parameter, β_{Eh}, is presented to express hysteretic energy indirectly. The β_{Eh} spectrum is constructed directly through subtracting the hysteretic energy of single degree-of-freedom (SDOF) system energy equation. The simplified β_{Eh} spectral formulation as well as pseudo-acceleration spectrum of modern seismic provisions is developed based on the regression analysis of the large number of seismic responses of SDOF system subjected to earthquake excitations, which considers the influence of earthquake event, soil type, damping ratio, and ductility factor. The relationship between PGV and PGA is established according to the statistical analysis relied on a total of 422 ground motion records. The combination of β_{Eh} spectrum and PGV/PGA equation allows determining the cumulative hysteretic energy as a main aseismic design indicator.

Keywords: nonlinear SDOF system; hysteretic energy; response spectrum; damping ratio; ductility

1. Introduction

The current seismic design philosophy followed in many earthquake-prone countries is still force based seismic design. This method can only take into account the effect of maximum response, however, the cumulative plastic cycle energy during the severe seismic excitations cannot be precisely considered (Fajfar and Vidic 1994). Housner (1956) suggested to develop a seismic design methodology based on energy criteria. Energy based seismic design considered that a structure can survive under a severe earthquake if the structural energy absorption capacity is greater than seismic input energy. This method is more advanced in that the accumulation of earthquake-induced damage can be taking into account reasonably. The energy-based seismic design approach is gaining extensive attention (Goel 1997, Leelataviwat *et al*. 2002, Choi *et al*. 2006, Teran-Gilmore *et al*. 2010, Sahoo and Chao 2010, Kharmale and Ghosh 2013, Habibi *et al*. 2013, Khampanit *et al*. 2014, Heidari and Gharehbaghi 2015). According to the energy concept and energy balance equation, the seismic input energy imparted to a structure is equal to the sum of kinetic energy, elastic strain energy, damping energy, and energy dissipation by hysteretic behavior of the components. The hysteretic energy is related to the structural damage, so it should be considered as much more reasonable design parameter. Therefore, the construction of hysteretic energy spectrum becomes the most important work.

In earlier researches, some researchers (e.g., Kato and Akiyama 1975, Fajfar and Fischinger 1990, Uang and Bertero 1990) considered the input energy was a very stable parameter of the structural response, and it hardly depended on the structural properties. The hysteretic energy spectrum could be obtained through the relationship between input energy and hysteretic energy indirectly (Fajfar and Vidic 1994). Akiyama (1985, 1988) and Surahman (2007) adopted the part of energy attributed to structural damage as design indicator, which could be computed from input energy through subtracting the damping energy. Decanini and Mollaioli (2001) firstly proposed a procedure for determining inelastic design earthquake input energy spectrum considering the influence of ductility, soil type, source-to-site distance, and magnitude. Subsequently, the spectrum of the hysteretic to input energy ratio was constructed for different soil types and target ductility ratios. López-Almansa *et al*. (2013) also proposed the design input energy spectra in terms of an equivalent velocity based on the Turkish strong ground motion records, in which the soil type, surface magnitude Ms, and the relevance of the near-source effect were considered. The empirical criteria for estimating the hysteretic energy from the design input energy were suggested. Bruneau and Wang (1996) proposed the normalized hysteretic energy spectrum based on the simple rectangular pulse and sine-wave ground excitations. Riddell and Garcia (2001) studied the inelastic response of single degree-of-freedom (SDOF) systems subjected to earthquake motions, and proposed a new method to derive hysteretic energy dissipation spectrum. Manfredi (2001) obtained the hysteretic energy spectrum from the knowledge of the pseudo-velocity spectrum, and introduced an important parameter I_D to estimate the cyclic work required by an earthquake. Chou and Uang (2000) established an attenuation relationship of the absorbed energy based on a total of 273 ground motion records from 15 significant earthquakes in California, and some important influencing factors, including earthquake

*Corresponding author, Associate Professor
E-mail: sungh-529@163.com

ISSN: 2092-7614 (Print), 2092-7622 (Online)

Table 1 The statistics of earthquake records

Soil type	Subset	Earthquake event	Date	Source magnitude M	Number of records	Average of site-source distance R(km)	Average of PGA (g)	Average of PGV (cm/s)	Average of PGD (cm)
S1 V_{s30}≥750 m/s	S1-Set 1	Anza (Horse Cany)	1980/02/25	4.9	4	8.9	0.11	3.30	2.21
	S1-Set 2	Cape Mendocino	1992/04/25	7.1	2	8.5	1.27	84.7	26.70
	S1-Set 3	Chi-Chi, Taiwan	1999/09/20	7.6	60	97.94	0.04	6.76	6.47
	S1-Set 4	Coyote Lake	1979/08/06	5.7	2	9.3	0.12	5.85	1.00
	S1-Set 5	Duzce, Turkey	1999/11/12	7.1	2	30.2	0.04	8.15	8.88
	S1-Set 6	Hollister	1974/11/28	5.4	2	10	0.12	3.35	0.15
	S1-Set 7	Kocaeli, Turkey	1999/08/17	7.4	6	28.57	0.14	24.25	18.83
	S1-Set 8	Landers	1992/06/28	7.3	8	59.15	0.23	21.34	15.04
	S1-Set 9	Loma Prieta	1989/10/18	6.9	18	62.62	0.11	11.36	3.87
	S1-Set 10	Lytle Creek	1970/09/12	5.4	2	20.6	0.06	1.50	0.09
	S1-Set 11	Morgan Hill	1984/04/24	6.2	2	16.2	0.08	2.90	1.14
	S1-Set 12	Northern Calif	1975/06/07	5.7	2	28.9	0.15	4.00	0.13
	S1-Set 13	Northridge	1994/01/17	6.7	16	41.33	0.29	16.91	3.60
	S1-Set 14	N. Palm Springs	1986/07/08	6.0	8	48.08	0.09	2.91	0.44
	S1-Set 15	San Francisco	1957/03/22	5.3	2	8.00	0.10	4.25	0.31
	S1-Set 16	San Fernando	1971/02/09	6.6	4	55.05	0.08	2.88	0.87
	S1-Set 17	Whittier Narrows	1987/10/01	6.0	8	18.80	0.15	6.93	0.72
S2 360~750 m/s	S2-Set 1	Cape Mendocino	1992/04/25	7.1	2	33.80	0.21	6.85	0.48
	S2-Set 2	Chi-Chi, Taiwan	1999/09/20	7.6	10	46.41	0.08	16.12	13.00
	S2-Set 3	Coyote Lake	1979/08/06	5.7	2	3.60	0.38	36.85	5.81
	S2-Set 4	Duzce, Turkey	1999/11/12	7.1	6	14.63	0.08	11.63	9.45
	S2-Set 5	Friuli, Italy	1976/09/15	5.5	4	15.85	0.17	8.75	1.13
	S2-Set 6	Hollister	1986/01/26	5.4	2	14.90	0.07	7.30	1.49
	S2-Set 7	Kobe	1995/01/16	6.9	2	0.6	0.71	77.80	18.82
	S2-Set 8	Kocaeli, Turkey	1999/08/17	7.4	5	27.80	0.17	30.34	26.92
	S2-Set 9	Landers	1992/06/28	7.3	12	134.42	1.78	2.51	1.95
	S2-Set 10	Livermore	1980/01/24	5.8	4	29.80	0.04	4.08	0.77
	S2-Set 11	Loma Prieta	1989/10/18	6.9	12	25.70	0.22	20.76	6.81
	S2-Set 12	Lytle Creek	1970/09/12	5.4	4	61.60	0.10	5.75	0.47
	S2-Set 13	Morgan Hill	1984/04/24	6.2	8	20.53	0.12	9.68	1.93
	S2-Set 14	Northridge	1994/01/17	6.7	24	41.52	0.44	29.80	11.79
	S2-Set 15	N. Palm Springs	1986/07/08	6.0	8	53.30	0.12	5.25	0.53
	S2-Set 16	Parkfield	1966/06/28	6.1	2	14.70	0.06	6.30	3.06

Table 1 Continued

Soil type	Subset	Earthquake event	Date	Source magnitude M	Number of records	Average of site-source distance R(km)	Average of PGA (g)	Average of PGV (cm/s)	Average of PGD (cm)
S2 360~750 m/s	S2-Set 17	San Fernando	1971/02/09	6.6	8	36.10	0.20	10.93	1.99
	S2-Set 18	Whittier Narrows	1987/10/01	6.0	26	44.39	0.07	3.72	0.43
S3 180~360 m/s	S3-Set 1	Chi-Chi, Taiwan	1999/09/20	7.6	8	83.53	0.10	18.35	11.57
	S3-Set 2	Coalinga	1983/05/02	6.4	2	47.30	0.14	10.40	1.18
	S3-Set 3	Coyote Lake	1979/08/06	5.7	2	31.20	0.04	3.50	0.38
	S3-Set 4	Imperial Valley	1979/10/15	6.5	2	11.10	0.40	25.25	4.18
	S3-Set 5	Landers	1992/06/28	7.3	6	142.23	0.05	7.37	2.11
	S3-Set 6	Livermore	1980/01/24	5.8	2	37.30	0.06	7.55	2.08
	S3-Set 7	Loma Prieta	1989/10/18	6.9	4	23.05	0.30	23.68	5.84
	S3-Set 8	Morgan Hill	1984/04/24	6.2	4	20.75	0.18	16.23	2.93
	S3-Set 9	Mt. Lewis	1986/03/31	5.6	2	15.50	0.15	13.45	3.03
	S3-Set 10	Northridge	1994/01/17	6.7	18	39.74	0.21	22.89	4.79
	S3-Set 11	Parkfield	1966/06/28	6.1	2	5.30	0.40	23.25	4.49
	S3-Set 12	San Fernando	1971/02/09	6.6	2	48.10	0.09	7.35	1.52
	S3-Set 13	Victoria, Mexico	1980/06/09	6.4	2	58.30	0.08	8.40	2.35
	S3-Set 14	Whittier Narrows	1987/10/01	6.0	15	23.44	0.15	7.93	1.05
S4 V_{s30}<180 m/s	S4-Set 1	Chi-Chi, Taiwan	1999/09/20	7.6	32	43.67	0.10	33.82	27.60
	S4-Set 2	Duzce, Turkey	1999/11/12	7.1	2	193.30	0.03	7.25	4.30
	S4-Set 3	Imperial Valley	1979/10/15	6.5	4	13.60	0.19	25.10	10.88
	S4-Set 4	Kobe	1995/01/16	6.9	12	10.50	0.40	51.88	15.13
	S4-Set 5	Kocaeli, Turkey	1999/08/17	7.4	2	78.90	0.22	36.60	27.96
	S4-Set 6	Loma Prieta	1989/10/18	6.9	4	65.40	0.19	34.08	8.87
	S4-Set 7	Morgan Hill	1984/04/24	6.2	2	54.10	0.06	3.65	0.65
	S4-Set 8	Northridge	1994/01/17	6.7	2	12.30	0.15	7.65	1.87
	S4-Set 9	Superstitn Hills(B)	1987/11/24	6.7	2	27.10	0.14	13.10	3.20
	S4-Set 10	Westmorland	1981/04/26	5.8	2	10.10	0.19	14.35	3.39

magnitude, source-to-site distance, site class, and ductility factor, were considered in this regressive formula. Dindar *et al*. (2015) proposed the input and plastic energy demand spectra, which incorporate different soil types, elastic perfectly plastic constitutive model, 5% viscous damping ratio, different ductility levels, and varying seismic intensities. However, most of these studies have been conducted with either less earthquake records sample or not considered the effect of earthquake event. Specially, the hysteretic energy derived from E_i/E_h formula is related to the accuracy of input energy formula. Furthermore, some regressive formulas of hysteretic energy are too complex, not suitable to use in design.

The objective of this study is to present a simplified normalized hysteretic energy spectral formula, i.e., β_{Eh} spectrum, directly based on the nonlinear time history results, and account for a large number of earthquake records. To do this, the details of the definitions and characteristics of β_{Eh} spectrum are presented herein. The β_{Eh} spectrum is computed based on elasto-plastic model under a total of 422 earthquake records. The effects of earthquake event, soil type, damping ratio, ductility, and post stiffness ratio on the β_{Eh} spectrum are analyzed and discussed. Finally, the design formula of a simplified normalized hysteretic energy spectrum is proposed for adopting in energy-based seismic design.

2. Structural model and strong ground motion records

A simple SDOF system was used in this study, with the force-displacement relationship given by two non-linear models: elasto-plastic and bilinear. The strength deterioration and stiffness degrading were not considered in restoring force model. The restoring force models are shown in Fig. 1.

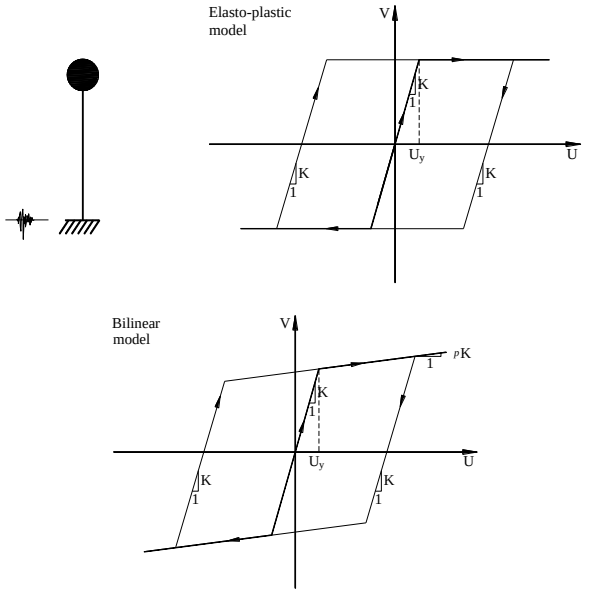

Fig. 1 Hysteretic models of SDOF

A total of 422 earthquake records were selected and classed from PEER database according to shear velocity. Table 1 lists the detailed information regarding the source magnitude, soil type, site-source distance, as well as PGA, PGV, and PGD. These records contain time histories ranging from a magnitude M=4.9 (Anza, Pinyon Flat, 1980) to a magnitude M=7.6 (Chi-Chi, Taiwan 1999), and whose distances from the site to source ranges from 0.3 to 194.1 km. Most of the records obtained from instrumental stations described as free-field, or located at ground level in small buildings.

3. Normalized hysteretic energy spectrum for SDOF system

The equation of motion for an inelastic SDOF system subjected to undirectional horizontal ground motion is

$$m\ddot{x} + c\dot{x} + f_s = -m\ddot{x}_g \tag{1}$$

where m is the mass; and c is the viscous damping coefficient; f_s is the restoring force; x_g and x are the ground displacement and relative displacement of the mass with respect to the base, respectively.

The energy equation can be derived from Eq. (1) through integrating over the entire duration of the earthquake (e.g., Kato and Akiyama 1975, Zahrah and Hall 1982), that is

$$\int_0^t m\ddot{x}\dot{x}dt + \int_0^t c\dot{x}\dot{x}dt + \int_0^t f_s\dot{x}dt = -\int_0^t m\ddot{x}_g\dot{x}dt \tag{2}$$

Eq. (2) can be rewritten as follows

$$E_{Kr} + E_D + E_E + E_H = E_{Ir} \tag{3}$$

where

$$E_{Kr} = \int_0^t m\ddot{x}\dot{x}dt; \quad E_D = \int_0^t c\dot{x}\dot{x}dt;$$
$$E_E + E_H = \int_0^t f_s\dot{x}dt; \quad E_{Ir} = -\int_0^t m\ddot{x}_g\dot{x}dt$$

Here E_{kr} represents the kinetic energy, which becomes null if the initial velocity is zero and the integration is carried out long enough until the system comes to rest; E_D is the energy dissipated by the viscous damping; E_E is the elastic strain energy stored in SDOF system; E_H is defined as the hysteretic energy, which dissipated by inelastic behavior; E_{Ir} denotes the total input energy introduced by the earthquake.

E_H is related to the damage of structure, and can be expressed in terms of the equivalent pseudo-velocities, V_{Eh}, which is defined as follows

$$V_{Eh} = \sqrt{\frac{2E_H}{m}} \tag{4}$$

In order to have a general dimensionless hysteretic energy measure, the equivalent velocity of hysteretic energy, V_{Eh}, can be normalized by dividing the peak ground

velocity (PGV) of earthquake excitation

$$\beta_{\mathrm{Eh}} = \frac{V_{\mathrm{Eh}}}{PGV} \tag{5}$$

Where PGV is the peak ground velocity of earthquake wave; β_{Eh} is dynamic magnification ratio based on the hysteretic energy.

Through changing the period of SDOF system, the cumulative hysteretic energy and β_{Eh} spectrum are computed and constructed based on the nonlinear time history analysis.

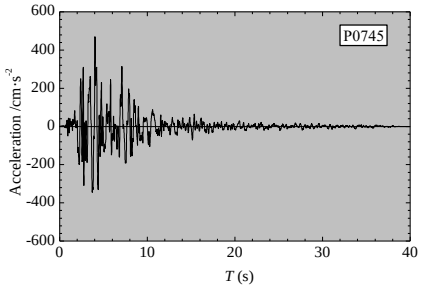

(a) The acceleration of earthquake wave-P0745

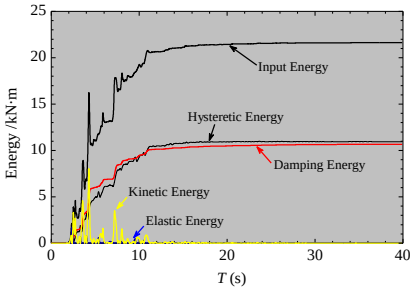

(b) energy composition

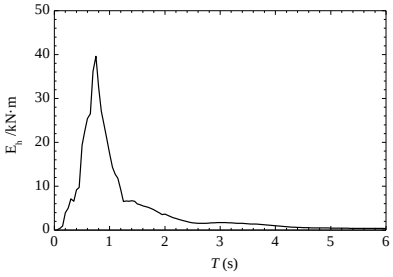

(c) hysteretic energy spectrum

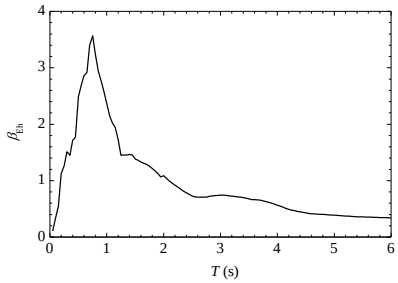

(d) normalized hysteretic energy spectrum

Fig. 2 The construction of normalized hysteretic energy spectrum based on a typical earthquake wave

Fig. 2 shows the time history of acceleration, energy composition, hysteretic energy, and β_{Eh} spectrum, according to a typical earthquake wave.

4. Influence factor analyses on the normalized hysteretic energy spectrum

The normalized hysteretic energy spectrum represented by Eqs. (1) to (5) is controlled by some primary factors. In order to determine the main influencing parameters, the following aspects of earthquake and structural characteristics are then investigated, including earthquake event, soil type, damping ratio, ductility, and post-stiffness ratio. In the present study, design variable considered is the fundamental period of the structure.

4.1 Influence of earthquake event

It is well known that earthquake event has a certain effect on the results of seismic response. Specially, when many ground records are taking from one earthquake event, the structural seismic response is mainly rely on this earthquake, and the contribution of other earthquake characters is weakened. To evaluate this earthquake event bias, two methods are adopted:

Method I: The seismic response of each earthquake record is used to represent an individual statistical sample, and conduct statistical analysis with other earthquake record result.

Method II: The mean seismic response of ground records from each earthquake with same soil type is used to represent this earthquake event, and conduct statistical analysis with other earthquake event result.

Fig. 3 compares the earthquake event effect on β_{Eh} spectrum from 422 selected earthquake records considering the different soil type.

The analysis results displayed in Fig. 3 indicate that earthquake event is an important influencing factor on the β_{Eh} spectrum. Plots from these figures show that the discrepancy of β_{Eh} analytical result based on two methods is very obvious except for soil S3 seismic response. The method I uses the seismic response of each earthquake record as an individual statistical sample, which leads to the average β_{Eh} spectrum significantly depending on the number of earthquake records from a certain earthquake event. For example, the subset named S1-set3 (Table 1) includes 60 earthquake records from Chi-Chi Taiwan (1999) earthquake event. When the method I is adopted, the seismic responses of 60 earthquake records will be regarded as 60 individual statistical samples, which results in the average β_{Eh} spectrum feature of soil S1 controlled by Chi-Chi earthquake event. However, the method II is different, because the average seismic response of 60 earthquake records is only regarded as an individual statistical sample. Thus, the effect of earthquake event for constructing β_{Eh} spectrum can be eliminated. Similarly, FEMA P-695 (2009) also suggests that no more than two of the strongest earthquake records are taken from each earthquake. Therefore, the method II proposed in this paper is much validated to take into account the effect of earthquake event.

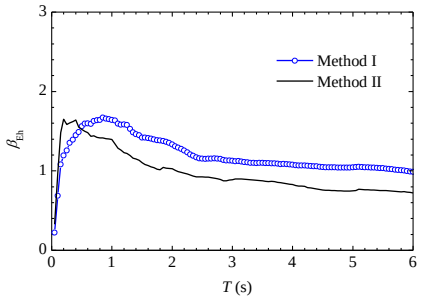

(a) soil S1

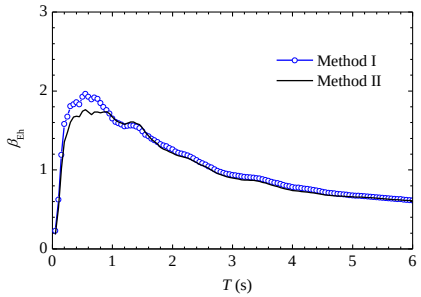

(b) soil S2

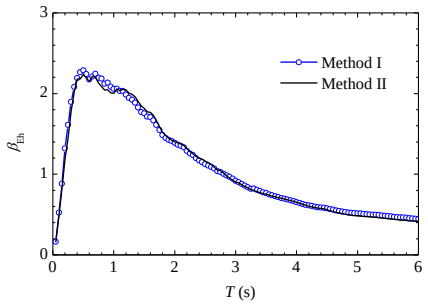

(c) soil S3

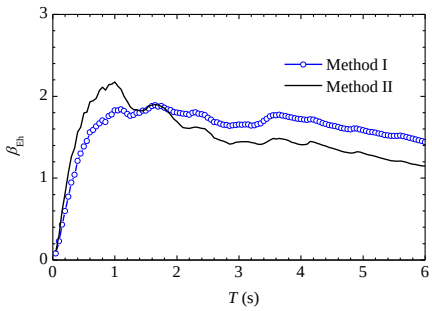

(d) soil S4

Fig. 3 The influence of earthquake event on β_{Eh} spectrum

4.2 Influence of soil type

In this section, the influence of soil type on the β_{Eh} spectrum was examined through considering the four soil classes S1, S2, S3, and S4. This results presented herein were based on the following parameters: elasto-plastic model, post stiffness ratio=0.00, μ=2, and damping ratio=5%. Fig. 4(a) allows comparing the trend of the mean β_{Eh} spectrum, and Fig. 4(b) depicts the variation coefficients of β_{Eh} spectra with different soil type.

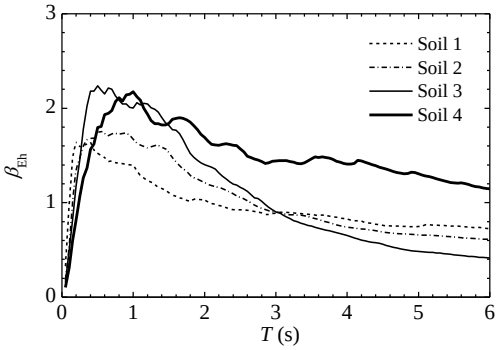

(a) mean normalized hysteretic energy spectrum

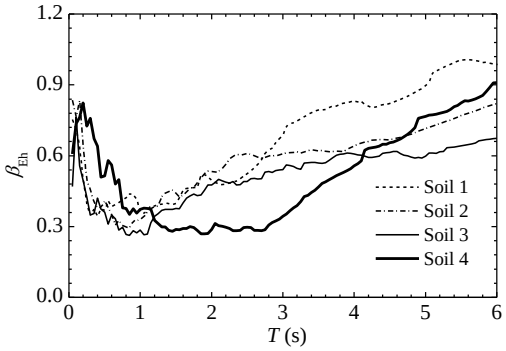

(b) variation coefficients

Fig. 4 The influence of soil type

As it can be seen, Fig. 4(a) indicates that soil type produces a significant influence on β_{Eh} spectral shape. The four spectral shapes are notably different from one another. The maximum values of β_{Eh} spectrum are close to 1.65 for soil S1, 1.75 for S2, 2.2 for S3, and 2.1 for S4. Generally, the peak of β_{Eh} tends to move toward the zone of low frequencies as the soil condition becomes soft. From the examination of all the mean normalized hysteretic energy spectrum, the first turning period depends strongly on the soil condition, and can be approximately taken as 0.15, 0.25, 0.4, and 0.5s, respectively, for the soil S1, S2, S3, and S4.

The knowledge of the coefficient of variation (COV) allows comparing the degree of uncertainty involved in the estimation of β_{Eh} spectrum. As shown in Fig. 4(b), it can be recognized the dispersion is generally considerable. For this parameter COV varies from a minimum of 0.26 to a maximum of 1. The soil type has a certain influence on the values of the variation coefficient.

4.3 Influence of damping ratio

The total energy imparted to the inelastic SDOF system by earthquake excitation is dissipated by damping and inelastic deformation. In order to investigate the influence of the damping on the β_{Eh} spectral shapes, the following analysis has been carried out and the results are shown in Fig. 5.

In Fig. 5, the distribution of β_{Eh} for soil S2 and μ=2 is presented. This analysis put in evidence that the value of β_{Eh}

tends to decrease as the damping ratio increase. Specially, such phenomenon was observed essentially during the high frequency region. The curve of β_{Eh} tends to more smooth with the damping ratio increasing. Normally, the character period of earthquake record is almost in the range of high frequency region, which leads to the resonance of SDOF system with similar frequency or period, and produces greater dynamic response. It is generally known that the damping ratio has an important role of reducing the peak, and makes the curve smoother. For low frequency region, the reducing peak function of damping ratio is not obvious except for decreasing the response of SDOF system. Generally, when the similar input energy imparts to the structure subjected to earthquake excitations, the energy dissipation due to damping ratio increases with the increase of damping ratio, and the energy dissipation of structural components due to inelastic deformation decreases obviously.

4.4 Influence of ductility

This analysis of the ductility effect on the β_{Eh} spectral shapes has been carried out for the soil S2 and for a ductility from 1.5 to 6, which is a reasonable range of ductility factor implicit in current seismic design, illustrated in Fig. 6.

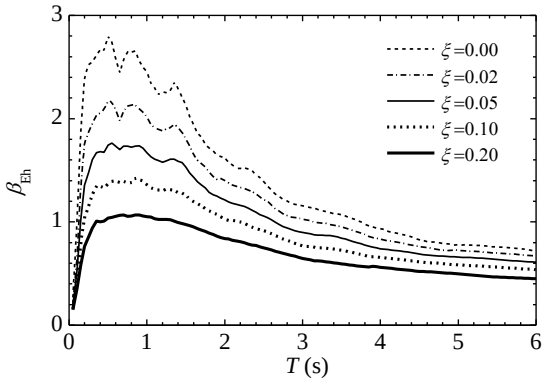

Fig. 5 The influence of damping ratio on the mean β_{Eh} spectrum: p=0, μ=2, soil S2

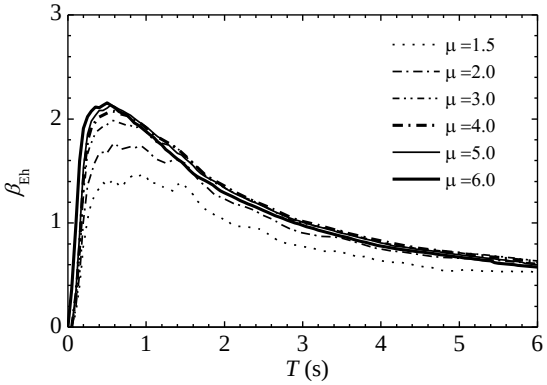

Fig. 6 The influence of ductility on the mean β_{Eh} spectrum: p=0, ξ=5%, soil S2

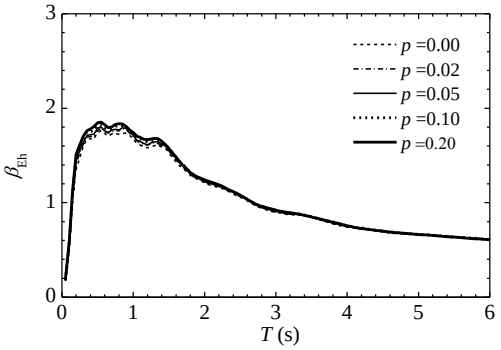

Fig. 7 The influence of post-stiffness on the mean β_{Eh} spectrum: μ=2, ξ=5%, soil S2

In Fig. 6, ductility is found to have an important effect on the β_{Eh} spectral shapes, and a clear trend was detected, i.e., the value of β_{Eh} spectrum is lower for smaller ductility value than for larger ductility. In other word, the larger ductility factor also implies greater hysteretic energy dissipation. However, the increment of β_{Eh} spectrum becomes small gradually with the increase of ductility value. For instance, for an increase in ductility value from 2 to 3, and from 4 to 5, respectively, the maximum value of β_{Eh} increases from 1.76 to 1.99, and from 2.08 to 2.14.

4.5 Influence of post-stiffness ratio

The post-stiffness ratio of bilinear model has a certain effect on the absorbing energy of inelastic SDOF system. In order to evaluate this effect, Fig. 7 shows the influence of post-stiffness ratio on the β_{Eh} spectral shape based on the soil S2, ξ=5%, and μ=2.

As it can be seen, the β_{Eh} spectral shape is not sensitive to the post-stiffness ratio. When the post-stiffness ratio varies from 0 to 0.2, the maximum value of β_{Eh} spectrum varies from 1.76 to 1.85. Therefore, it seems that it appears reasonable to ignore the influence of post-stiffness, when proposing the formulation of β_{Eh} spectrum.

5. A simplified normalized hysteretic energy design spectrum

The normalized hysteretic energy spectral shape should be associated with simple mathematical expressions and smoothened curves. Based on the results of parameter analysis, the normalized hysteretic energy spectral shape is mainly associated with soil type, damping ratio, and ductility, except that the effect of post-stiffness can be ignored. Therefore, the mathematic formulation of β_{Eh} spectrum can be written as

$$\beta_{Eh} = f\left(T, \xi, \mu, S\right) \tag{6}$$

where T is the vibration period; ξ is the damping ratio; μ is the ductility; S is the soil type.

Referring to the research results of Decanini and Mollaioli (2001), the normalized design hysteretic energy spectral shape was individuated by smooth curves accounting for the fundamental trends and defined by

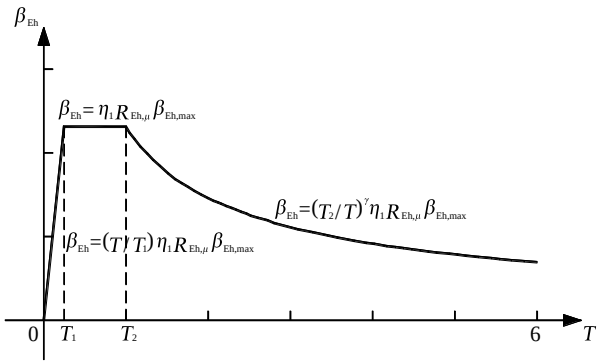

Fig. 8 Normalized hysteretic energy spectral shape

simple mathematical relationships. The graph of the adopted normalized hysteretic energy spectral shape, plotted in Fig. 8, consists of three regions characterized by the following patterns:

1. Linear variation for the high frequencies;
2. A constant branch for the intermediate frequencies;
3. A decaying curve for the low frequencies.

The β_{Eh} spectrum can be written in the following equations

$$\begin{aligned} \beta_{Eh} &= \left(\frac{T}{T_1}\right)\eta_1 R_{Eh,\mu}\beta_{Eh,max} && 0 \le T < T_1 \\ \beta_{Eh} &= \eta_1 R_{Eh,\mu}\beta_{Eh,max} && T_1 \le T < T_2 \\ \beta_{Eh} &= \left(\frac{T_2}{T}\right)^{\eta}\eta_1 R_{Eh,\mu}\beta_{Eh,max} && T_2 \le T \le 6s \end{aligned} \tag{7}$$

Where, T_1 represents the period corresponding to the beginning of the constant region of the spectrum, and T_2 is the period corresponding to the beginning of the decaying branch; $\beta_{Eh,max}$ is the maximum spectral value relative to the constant region of the β_{Eh} spectrum; γ is the decaying parameter, which is relate to the damping ratio, and can be determined in Eq. (8)

$$\gamma = \gamma_1 + \frac{0.05-\xi}{0.3+6\xi} \tag{8}$$

A simplified formulation of Eq. (9) was proposed to consider the effect of damping ratio, which is equal to

$$\eta_1 = 1 + \frac{0.05-\xi}{0.1+1.5\xi} \tag{9}$$

Ductility has a significant effect on the β_{Eh} spectral shape, and then the following expression can be derived

$$R_{Eh,\mu} = 1 + \frac{\mu-1.5}{1.6\mu} \tag{10}$$

T_1, T_2, γ_1 and $\beta_{Eh,max}$ depend on the soil type, which can be determined in Table 2. The period T_1, corresponding to beginning of the plateau (region 2), is taken as the first turning period, which is equal to 0.15, 0.25, 0.4, and 0.5s, respectively for the soil S1, S2, S3, and S4, fairly similar to that suggested by Decanini and Mollaioli (2001). The period T_2, corresponding to the end of the constant branch (region 2), is equal to the second turning period determined by the mathematical fitting method. The original average β_{Eh} spectrum is firstly fitted through the simplified three-region mathematical formulas. When the correlation coefficient (R^2) of the two curves is the largest, the second turning period is recorded as T_2.

The parameter, $\beta_{Eh,max}$, represents the maximum value of β_{Eh} and characterizes the constant range of the spectral shape. The average value of β_{Eh} between T_1 and T_2 is computed, and the maximum of average β_{Eh} is used as a representative value of $\beta_{Eh,max}$. Fig. 9 illustrates the distribution of β_{Eh} between T_1 and T_2 for different soil type.

Table 2 Parameters $\beta_{Eh,max}$,T_1 and T_2 depending on soil type

Soil type	$\beta_{Eh,max}$	γ_1	T_1	T_2
S1	1.35	0.45	0.15	0.8
S2	1.45	0.60	0.25	1.0
S3	1.85	1.00	0.40	1.2
S4	1.75	0.35	0.50	1.4

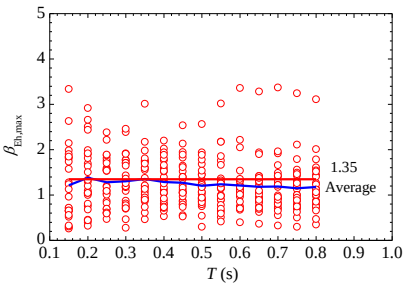

(a) soil S1

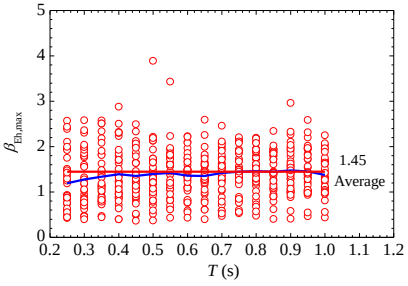

(b) soil S2

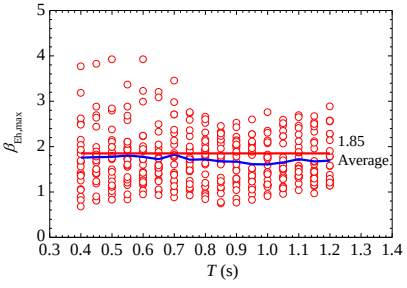

(c) soil S3

Fig. 9 The determination of $\beta_{Eh,max}$: (a) soil S1; (b) soil S2; (c) soil S3; and (d) soil S4

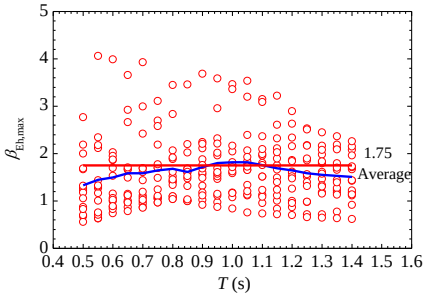

(d) soil S4

Fig. 9 Continued

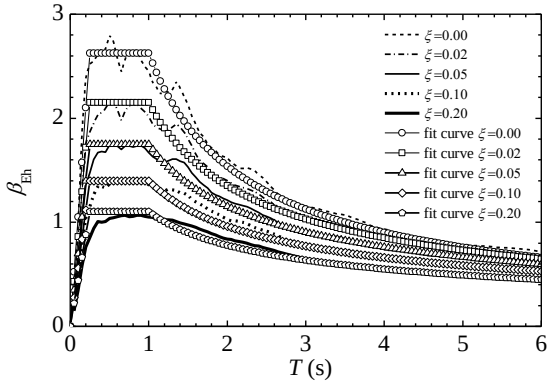

Fig. 10 Comparison between β_{Eh} spectral shape from Eq. (7) and the mean spectra calculated by 141 real earthquake waves of S2 soil condition for μ=2, and P=0

5.1 The verification of simplified β_{Eh} spectrum formula considering damping ratio

The β_{Eh} spectral shape calculated by Eq. (7) has been compared with the mean value calculated by 141 real earthquake waves of S2 soil condition, considering the different damping ratio, for μ=2, and P=0, as illustrated in Fig. 10.

5.2 The verification of simplified β_{Eh} spectrum formula considering ductility

The ductility is another significant parameter, and Eq. (10) is used to reflect ductility effect. In Fig. 11, the reasonability of Eq. (10) is evaluated, and compares the proposed β_{Eh} spectra with the mean value calculated by 141 real earthquake waves of S2 soil condition, considering the ductility, for ξ=5%, and P=0.

5.3 The verification of simplified β_{Eh} spectrum formula considering soil type

Fig. 12 reports the β_{Eh} spectral shape calculated by Eq. (7), and compares with the mean value calculated by four sets earthquake waves from four soil types, for ξ=5%, μ=2, and P=0.

As it can be noticed from Fig.10 to Fig.12, the spectral shapes of fit curves agree well with the shapes of the mean

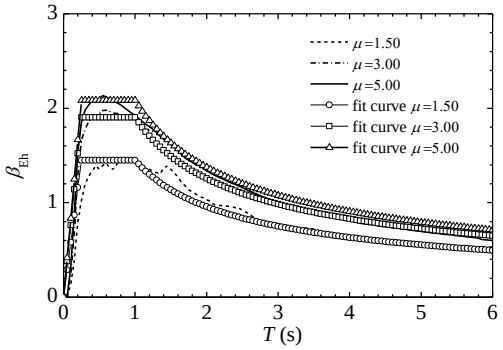

(a) μ=1.5, 3, and 5

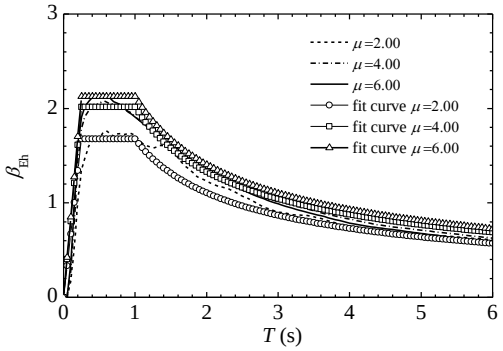

(b) μ=2, 4, and 6

Fig. 11 Comparison between β_{Eh} spectral shape from Eq. (7) and the mean spectra calculated by 141 real earthquake waves of S2 soil condition for ξ=5%, and P=0

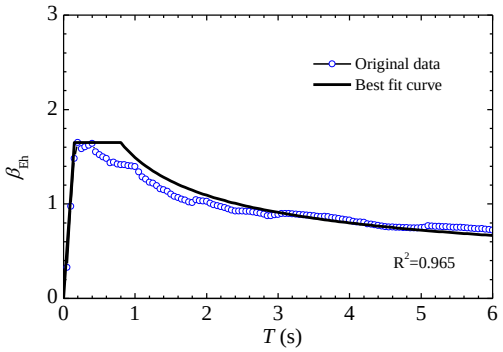

(a) soil S1

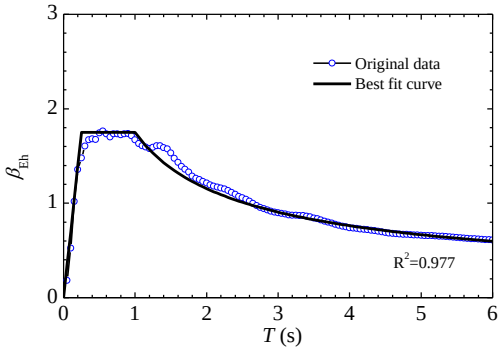

(b) soil S2

Fig. 12 Comparison between β_{Eh} spectra shape from Eq. (7) and the mean spectra calculated from four soil types

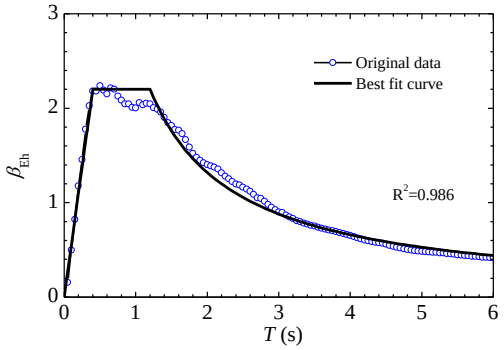

(c) soil S3

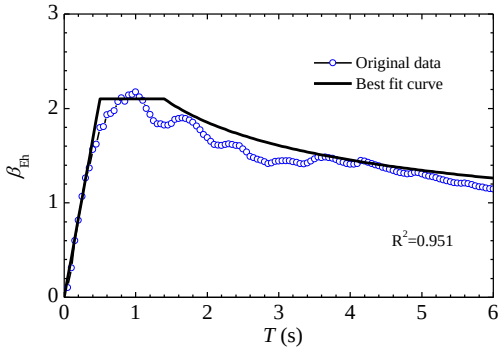

(d) soil S4

Fig. 12 Continued

β_{Eh} spectra calculated from four soil types. The Eq. (7) can reasonably reflect all kinds of influencing factor, including damping ratio, ductility, and soil type, whether in the high-frequency region or low-frequency region. The β_{Eh} spectrum can be expressed in Eq. (7), and used in energy-based seismic design.

6. Seismic design parameter value representing by PGV

As previously mentioned, hysteretic energy is a stable indicator for representing the seismic demand, while Eq. (7) can be used to determine the β_{Eh} spectral value. The β_{Eh} is the ratio of the equivalent velocity of hysteretic energy to the peak ground velocity of earthquake wave. Hence, seismic design parameter value based on PGV parameter need to be determined to compute the V_{Eh}. However, the main problem is that most seismic provisions adopt the force-based seismic design method, and use PGA or spectral acceleration as seismic design indicator, not velocity or PGV parameter. Therefore, the relationship between PGA and PGV need to be constructed in order to keep the same seismic design level with current seismic code. The relationship between PGV and PGA is established according to the statistical analysis relied on a total of 422 ground motion records.

In Fig. 13, the PGV/PGA ratios of all the records used in the analysis are drawn, where the mean value and the mean-plus-one-standard-deviation of PGV/PGA ratio are calculated.

On the basis of statistical analysis, the relative formula between PGV and PGA has been regressed and proposed

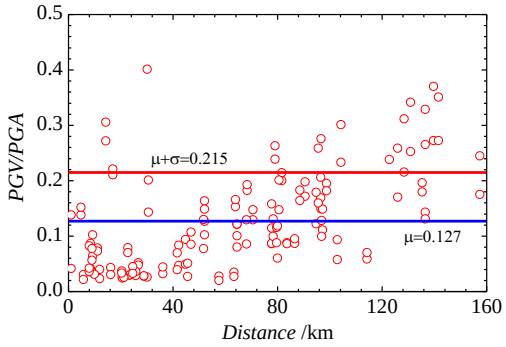

(a) soil S1

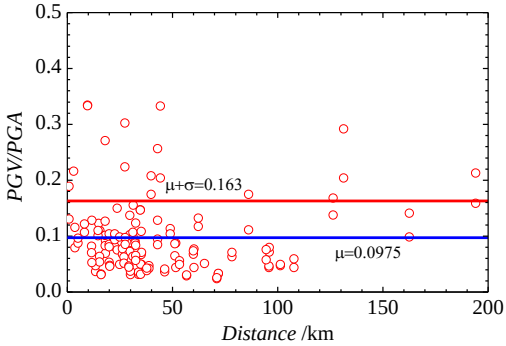

(b) soil S2

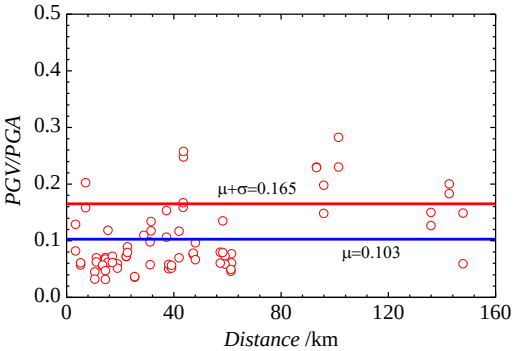

(c) soil S3

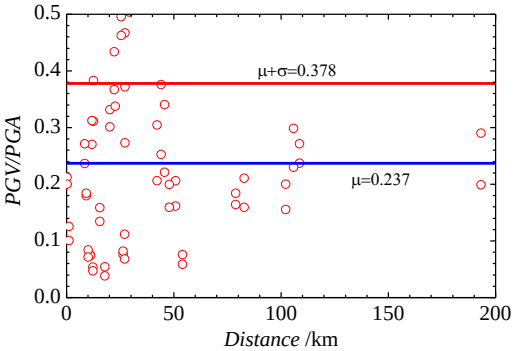

(d) soil S4

Fig. 13 The PGV/PGA ratios of all the records used in this analysis

$$\frac{P\hat{G}V}{P\hat{G}A}=1.6\frac{\overline{PGV}}{\overline{PGA}} \tag{11}$$

Where $\overline{PGV}/\overline{PGA}$ is the mean ratio of peak ground velocity and peak ground acceleration of original real earthquake records; $P\hat{G}A$ is the design peak ground acceleration under the earthquake design level provided by current seismic specification; $P\hat{G}V$ is the design peak ground velocity having the same design level with $P\hat{G}A$. The constant 1.6 is obtained by fit $\overline{PGV}/\overline{PGA}$ ratio to the mean-plus-one-standard-deviation of Table 3.

With reference to Fig. 13, it is obviously that there is not direct relationship between PGV and PGA of earthquake records. So, the mean and standard deviation of PGV/PGA are computed based on statistical analysis. The mean of PGV/PGA for different soil type is 0.127, 0.098, 0.103 and 0.237, and standard deviation is 0.088, 0.065, 0.062 and 0.141, respectively. The mean value plus a standard deviation of PGV/PGA is used to construct the statistical regression formula. For simplification, the mean of PGV/PGA parameter is defined to 0.13, 0.1, 0.1, and 0.24 for soil S1 to S4. In Table 3, the PGV/PGA according to the statistical analysis is calculated based on the proposed mean value of PGV/PGA, and the guaranteeing probability of calculating value is approximately 80%.

The seismic design level of Chinese seismic specification (GB50011-2010) is provided in Table 4. According to Eq. (11) and Table 4, $P\hat{G}V$ can be obtained, consisting with the same seismic design level representing $P\hat{G}A$ in Chinese seismic specification.

Fig. 14 illustrates the equivalent velocity spectra of hysteretic energy for given values of ξ=5%, μ=2, and P=0 with different seismic intensity under 2%~3% probability of exceedance in 50 years. With reference to Fig. 14, an energy combination approach (Kalkan 2006) according to the first several structural periods is used to generate total structural hysteretic energy, which can be adopted in energy-based seismic design.

Table 3 The statistical data of PGV/PGA

Soil type	$\overline{PGV}/\overline{PGA}$ (The mean of PGV/PGA)		Standard Deviation	PGV/PGA	$1.6\overline{PGV}/\overline{PGA}$ (based on μ)	Guaranteeing Probability
	μ	μ	σ	$\mu+\sigma$		
S1	0.127	0.13	0.088	0.215	0.208	82.12%
S2	0.098	0.1	0.065	0.163	0.160	83.01%
S3	0.103	0.1	0.062	0.165	0.160	82.11%
S4	0.237	0.24	0.141	0.378	0.384	85.15%

Table 4 The maximum PGA in time history analysis of Chinese seismic code (cm.s^{-2})

Seismic hazard level	seismic intensity of Zone 6 (cm.s^{-2})	seismic intensity of Zone 7 (cm.s^{-2})	seismic intensity of Zone 8 (cm.s^{-2})	seismic intensity of Zone 9 (cm.s^{-2})
63% probability of exceedance in 50 years	18	35(55)	70(110)	140
10% probability of exceedance in 50 years	50	100(150)	200(300)	400
2%~3% probability of exceedance in 50 years	125	220(310)	400(510)	620

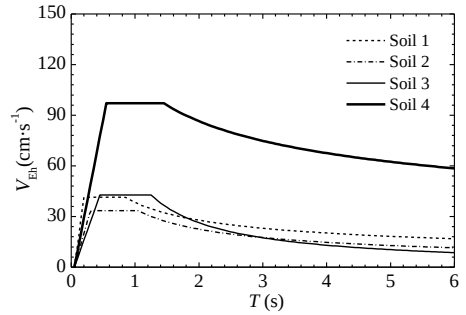

(a) seismic intensity of Zone 6

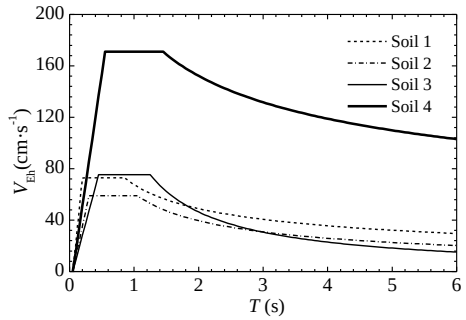

(b) seismic intensity of Zone 7

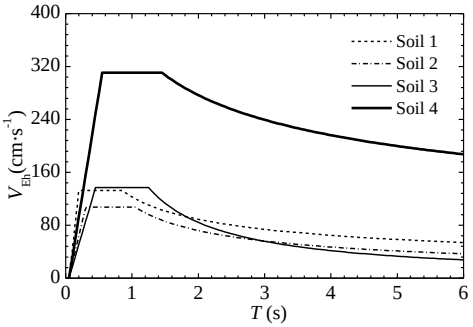

(c) seismic intensity of Zone 8

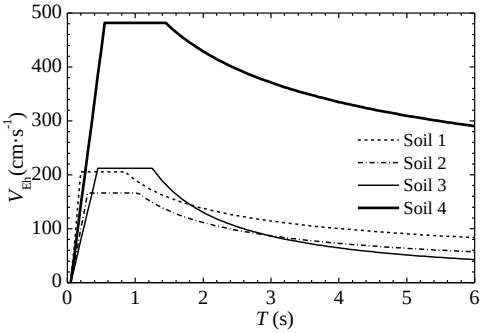

(d) seismic intensity of Zone 9

Fig. 14 Hysteretic energy spectra based on the regressive formula

7. Conclusions

In this paper, a simplified normalized hysteretic spectrum has been proposed for SDOF system subjected to earthquake excitations. The thoughts and conclusions are summarized as follows:

- The hysteretic energy relate to structural damage is an ideal design parameter in the energy-based seismic design. The dimensionless parameter, β_{Eh}, is presented to express structural hysteretic energy, and the computing method of normalized hysteretic energy spectrum is given in this paper.
- The effect of earthquake event, soil type, ductility, and damping ratio on the β_{Eh} spectrum is significantly considerable, which need to be taken into account constructing β_{Eh} spectrum. However, the post-stiffness ratio of nonlinear SDOF system is not sensitive to β_{Eh} spectrum, which can be ignored.
- The simplified mathematical formula of β_{Eh} spectrum as a function of structural period, damping ratio, and ductility. This formula can provide results generally in good agreement with the exact values.
- The relationship between PGV and PGA is proposed based on the statistical analysis of 422 earthquake records. According to Eq. (11), the seismic hazard level representing by PGV parameter can be obtained, which has the same seismic hazard level expressing by PGA indicator in current seismic code.

Acknowledgements

This research is part of a more comprehensive project supported by National Science Foundation of China (Grant No. 51578355 and 51278320), and Natural Science Foundation of JiangSu Province (Grant No. BK20151200). Any opinions, findings, and conclusions or recommendations expressed in this material are solely those of the authors and do not necessarily reflect the views of the sponsors.

References

Akiyama, H. (1985), *Earthquake Resistance Limit State Design for Buildings*, University of Tokyo Press, Tokyo, Japan.

Akiyama, H. (1988), "Earthquake resistant design based on the energy concept", *Proceedings of the 9th World Conference on Earthquake Engineering*, Tokyo, Japan.

Dindar, A.A., Yalçın, C., Yüksel, E., Özkaynak, H. and Büyüköztürk, O. (2015), "Development of earthquake energy demand spectra", *Earthq. Spectra*, **31**(3), 1667-1689.

Bruneau, M. and Wang, N. (1996), "Normalized energy-based methods to predict the seismic ductile response of SDOF structures", *Eng. Struct*., **18**(1), 13-28.

Chou, C.C. and Uang, C.M. (2000), "Establishing absorbed energy spectra-an attenuation approach", *Earthq. Eng. Struct. D*., **29**(10), 1441-1455.

Choi, H., Kim, J. and Chung, L. (2006), "Seismic design of buckling-restrained braced frames based on modified energy-balance concept", *Can. J. Civ. Eng*., **33**(10), 1251-1260.

Decanini, L.D. and Mollaioli, F.L. (1998), "Formulation of elastic earthquake input energy spectra", *Earthq. Eng. Struct. D*., **27**(12), 1503-1522.

Decanini, L.D. and Mollaioli, F.L. (2001), "An energy-based methodology for the assessment of seismic demand", *Soil. Dyn. Earthq. Eng*., **21**(2), 113-137.

Fajfar, P. and Fischinger, M.A. (1990), "Seismic procedure including energy concept", *Proceedings of IX ECEE*, Moscow, Vol.2, 312-321.

Fajfar, P. and Vidic, T. (1994), "Consistent inelastic design spectra: hysteretic and input energy", *Earthq. Eng. Struct. D*., **23**(5), 523-537.

FEMA P-695. (2009), "Quantification of building seismic performance factor", Federal Emergency Management Agency, Washington, DC, USA.

GB50011-2010. (2016), *Code for seismic design of buildings*, China Architecture and Building Press, Beijing, China.

Goel, R.K. (1997), "Seismic response of asymmetric system: energy-based approach", *J. Struct. Eng*., ASCE, **123**(11), 1444-1453.

Habibi, A., Chan, R.W.K. and Albermani, F. (2013), "Energy-based design method for seismic retrofitting with passive energy dissipation systems", *Eng. Struct*., **46**(1), 77-86.

Heidari, A. and Gharehbaghi, S. (2015), "Seismic performance improvement of special truss moment frames using damage and energy concepts", *Earthq. Eng. Struct. D*., **44**(7), 1055-1073.

Housner, G.W. (1956), "Limit design of structures to resist earthquakes", *Proceedings of the 1st World Conference Earthquake Engineering*., Berkeley, California, USA.

Kato, B. and Akiyama, H. (1975), "Energy input and damages in structures subjected to severe earthquakes", *Trans. Architec. Inst. Japan*, **235**, 9-18.

Kalkan, E. (2006), "Prediction of seismic demand in building structures", Ph.D. Dissertation, University of California at Davis.

Kharmale, S.B. and Ghosh, S. (2013), "Performance-based plastic design of steel plate shear wall", *J. Construct. Steel. Res*., **90**(5), 85-97.

Khampanit, A., Leelataviwat, S., Kochanin, J. and Warnitchai, P. (2014), "Energy-based seismic strengthening design of non-ductile reinforced concrete frames using buckling-restrained braces", *Eng. Struct*., **81**, 110-122.

Leelataviwat, S., Goel, S.C. and Stojadinović, B. (2002), "Energy-based seismic design of structures using yield mechanism and target drift", *J. Struct. Eng*., ASCE, **128**(8), 1046-1054.

López-Almansa, F., Yazgan, A. and Benavent-Climent, A. (2013), "Design energy input spectra for high seismicity regions based on Turkish registers", *Bull. Earthq. Eng*., **11**(4), 885-912.

Manfredi, G. (2001), "Evaluation of seismic energy demand", *Earthq. Eng. Struct. D*., **30**(4), 485-499.

Riddell, R. and Garcia, J.E. (2001), "Hysteretic energy spectrum and damage control", *Earthq. Eng. Struct. D*., **30**(12), 1791-1816.

Surahman, A. (2007), "Earthquake-resistant structural design through energy demand and capacity", *Earthq. Eng. Struct. D*., **36**(14), 2099-2117.

Sahoo, D.R. and Chao, S. (2010), "Performance-based plastic design method for buckling-restrained braced frames", *Eng. Struct*., **32**(9), 2950-2958.

Teran-Gilmore, A., Sanchez-Badillo, A. and Espinosa-Johnso, M. (2010), "Performance-based seismic design of reinforced concrete ductile buildings subjected to large energy demands", *Earthq. Struct*., **1**(1), 69-91.

Uang, C.M. and Bertero, V.V. (1990), "Evaluation of seismic energy in structures", *Earthq. Eng. Struct. D*., **19**(1), 77-90.

Zahrah, T. and Hall, W.J. (1982), "Seismic energy absorption in simple structures", Structural Research Series, No. 501, University of Illinois, Urbana, IL.

KT